



Published in final edited form as:

Nat Methods. 2023 May ; 20(5): 682–685. doi:10.1038/s41592-023-01819-w.

***In vivo* photopharmacology with a caged mu opioid receptor agonist drives rapid changes in behavior**

Xiang Ma^{1,†}, Desiree A. Johnson^{1,†}, Xinyi Jenny He¹, Aryanna E. Layden¹, Shannan P. McClain¹, Jean C. Yung¹, Arianna Rizzo^{2,3}, Jordi Bonaventura^{2,3}, Matthew R. Banghart^{1,*}

¹Department of Neurobiology, School of Biological Sciences, University of California San Diego, La Jolla, CA 92093, USA

²Departament de Patologia i Terapèutica Experimental, Institute de Neurociències, Universitat de Barcelona, L'Hospitalet de Llobregat, Catalonia, Spain

³Neuropharmacology & Pain Group, Neuroscience Program, Bellvitge Institute for Biomedical Research (IDIBELL), L'Hospitalet de Llobregat, Catalonia, Spain

Abstract

Photoactivatable drugs and peptides can drive quantitative studies into receptor signaling with high spatiotemporal precision, yet few are compatible with behavioral studies in mammals. We developed CNV-Y-DAMGO, a caged derivative of the mu opioid receptor-selective peptide agonist DAMGO. Photoactivation in the mouse ventral tegmental area produced an opioid-dependent increase in locomotion within seconds of illumination. These results demonstrate the power of *in vivo* photopharmacology for dynamic studies into animal behavior.

Photoactivatable ligands are powerful tools for probing receptor signaling in living systems^{1–3}. In the case of “caged” ligands, a photo-cleavable moiety is incorporated in a way that blocks activity until it is removed with light. Because photorelease is typically much faster than the biological processes under study, pre-equilibration of the caged molecule followed by photolysis can provide a robust stimulus that facilitates quantitative analysis of downstream processes. Although a few studies have achieved *in vivo* uncaging, none have demonstrated rapid responses that are desirable for studies into animal behavior^{4–8}.

The mu opioid receptor (MOR) is an inhibitory, G_{i/o}-coupled G protein-coupled receptor (GPCR) that is widely expressed in the nervous system. MORs are the primary target of opioid analgesics such as morphine and fentanyl, and are activated by endogenous opioid neuropeptides enkephalin, beta-endorphin and dynorphin⁹. How MOR activation in specific

*Correspondence to Matthew R. Banghart, mbanghart@ucsd.edu.

†Equal contribution

Author Contributions Statement

X.M., D.A.J., X.J.H., and M.R.B. designed research. X.M., D.A.J., A.E.L., X.J.H., S.P.M., J.C.Y., A.R., and J.B. performed research. X.M. contributed new reagents or analytical tools. X.M., D.A.J., X.J.H., and M.R.B. analyzed data. M.R.B., X.M., and D.A.J. wrote the paper.

Competing interests

The authors declare no competing financial interests.

brain regions acutely impacts circuit activity and behavior, and how this changes with experience or adaptation to opioid drug use, remains unclear. To facilitate studies into opioid receptor signaling in the nervous system, we previously developed several caged opioid ligands, including analogues of the neuropeptide agonists [Leu⁵]-enkephalin (LE) and dynorphin A (1–8) (Dyn8)^{10,11}. Although LE activates MORs with nanomolar affinity, it also activates delta opioid receptors (DORs) in a similar concentration range^{9,10}. In addition, because peptides such as LE and, by extension, its caged variants, are rapidly degraded *in vivo* ($t_{1/2} < 4$ min)¹², currently available forms of caged LE are not readily compatible with *in vivo* experiments that investigate the role of MOR signaling in neural circuit function and animal behavior.

To enable *in vivo* experiments involving rapid activation of endogenous MORs, we developed a caged analogue of the MOR-selective peptide agonist [D-Ala², N-MePhe⁴, Gly-ol]-enkephalin (DAMGO)¹³. As DAMGO is an enkephalin derivative that was designed to resist proteolysis, it shares a cageable pharmacophore with LE and Dyn8. Our caged DAMGO design is based on our prior success in caging LE (1, Fig. 1) by appending a caging group to the N-terminal tyrosine phenol to produce (carboxy-nitrobenzyl)-tyrosine-LE or CYLE (2)¹⁰. Given the structural similarity between DAMGO (3) and LE, we reasoned that caging this site would similarly reduce the affinity of DAMGO for MOR. We chose to use the carboxy-nitroveratryl (CNV) caging group, as it includes a negatively charged carboxylic acid to facilitate solubility, and because it is sensitive to commonly used ultraviolet (UV) and violet light sources. Importantly, we previously found that caging the N-terminal tyrosine in LE with the CNV group (CNV-Y-LE) afforded rapid photorelease in brain slices to activate MORs with good sensitivity to UV light¹¹.

Our three-step synthesis involves selective functional group modifications of commercially available DAMGO (3) to afford milligram quantities of CNV-Y-DAMGO (4) in ~45% overall yield (Extended Data Fig. 1). We evaluated the activity of CNV-Y-DAMGO at MORs using a cAMP assay of G_α signaling in HEK293T cells (Fig. 1B). Whereas we found the EC₅₀ of commercial DAMGO to be 1.5 nM in this assay, the EC₅₀ of CNV-Y-DAMGO was 1.7 μM, which indicates that inactive concentrations of CNV-Y-DAMGO should be photoconverted to near saturating concentrations of DAMGO. CNV-Y-DAMGO did not exhibit agonism at the delta (DOR) and kappa (KOR) opioid receptors, or the nociception/orphanin FQ receptor (NOP), nor did it activate β-arrestin signaling at MOR (Extended Data Fig. 2). We confirmed that CNV-Y-DAMGO cleanly releases DAMGO in aqueous solution by mass spectrometry, that it is stable in the dark for at least 24 h, and found that it undergoes photolysis at a rate ~2.25x that of MNI-glutamate, a caged glutamate derivative commonly used in brain slices, and that its UV/VIS spectrum changes upon photolysis (Extended Data Fig. 3).

To validate CNV-Y-DAMGO at native opioid receptors, we performed whole-cell voltage clamp recordings in mouse hippocampal brain slices, where electrically-evoked synaptic inhibition in the perisomatic region of CA1 pyramidal neurons is strongly suppressed by both MOR and DOR agonists^{11,14} (Fig. 1C). We first verified the inactivity of CNV-Y-DAMGO by recording inhibitory post-synaptic currents (IPSCs). Whereas bath application of DAMGO (1 μM) suppressed IPSC amplitude by ~70%, CNV-Y-DAMGO (1 μM) had no

discernable effect on synaptic transmission (Fig. 1D) (DAMGO: mean 0.70 ± 0.02 SEM; CNV-Y-DAMGO: mean -0.046 ± 0.05 SEM; $p < 0.0001$, Mann-Whitney test). We next found that 5 ms flashes of 355 nm light (84 mW measured at the back aperture), applied 2 sec prior to an electrical stimulus, rapidly suppressed inhibitory synaptic transmission, and that this reversed over the course of several minutes (Fig. 1E). Consistent with MOR activation, the selective MOR antagonist CTAP completely blocked the optically-evoked suppression of synaptic transmission (Fig. 1F) (CNV-Y-DAMGO + UV: mean 0.61 ± 0.05 SEM; CNV-Y-DAMGO + UV + CTAP: mean -0.05 ± 0.10 SEM, $p = 0.001$, Mann-Whitney test).

We pursued *in vivo* uncaging using optofluidic cannulas that deliver liquid and light to the same site, implanted above the left nucleus accumbens medial shell (NAc-mSh), where MOR agonists are rewarding, reinforce food consumption, and suppress pain-related behavior^{15,16} (Fig. 2A). We asked if CNV-Y-DAMGO photoactivation modulates the behavioral response to an injection of formalin (2.5%), an irritant that produces inflammatory pain, into the contralateral (right) hindpaw. We quantified the formalin-evoked biting and licking behavior as the time spent attending to the inflamed paw (5 min bins), before and after infusion of CNV-Y-DAMGO (200 μ M, 0.5 μ l) and subsequent application of a train of 375 nm light flashes (10×200 ms flashes, 1 Hz, 70 mW). To control for the effect of tethering on the paw attending behavior, we used mice implanted with a standard optical fiber in the prefrontal cortex. Formalin injection produced an acute, transient increase in paw attending, followed by a quiet phase and a tonic phase (Fig. 2B). Compared to the tethered control condition, CNV-Y-DAMGO photoactivation in the NAc-mSh just before the peak of the tonic phase produced a sharp decrease in paw attending that lasted for at least 10–20 min (Supplementary Videos 1 and 2). This result demonstrates the feasibility of using *in vivo* opioid peptide uncaging to manipulate and study behavior.

To establish the temporal precision of *in vivo* uncaging with CNV-Y-DAMGO, we implanted male and female mice with optofluidic cannula over the left ventral tegmental area (VTA, Fig. 2C), where MOR agonists activate dopamine neurons through a disinhibitory mechanism¹⁷. This is accompanied by an increase in locomotion that can be measured with good temporal resolution¹⁸. Based on experiments with DAMGO in which locomotor activity peaked 10–20 min post-infusion (Extended Data Fig. 4), we applied flashes of 375 nm light 15 min after infusion of CNV-Y-DAMGO (200 μ M, 0.5 μ l). For each mouse, we quantified both the instantaneous velocity (5 second bins), and the distance travelled in 15-minute windows before and after light application.

Pairing CNV-Y-DAMGO infusion with strong UV illumination (10×200 ms flashes, 1 Hz, 70 mW) produced a rapid increase in movement velocity that lasted over 25 min (Fig. 2D, E). Systemic administration of the opioid antagonist naloxone (NLX, 3 mg/kg) strongly attenuated the locomotor response to DAMGO photorelease (Supplementary Videos 3 and 4). Importantly, light alone had no effect on movement velocity, and CNV-Y-DAMGO did not exhibit any residual activity at this dose when illumination was omitted (Fig. 2F and Extended Data Fig. 4). A less intense optical stimulus (1×200 ms flash, 70 mW) produced a smaller, transient increase in locomotor behavior (Fig. 2G). Locomotion increased within one second after the flash, reaching a transient steady state within 2 seconds (Fig. 2H).

This result reveals that endogenous opioid receptors can rapidly modulate neural circuit function and behavior on the timescale of seconds while demonstrating the power of using light-activated drugs for behavioral pharmacology experiments.

In vivo photopharmacology is currently an area of great research interest^{2,3,19,20}. A growing number of studies have used photoswitchable ligands to manipulate both genetically engineered and endogenous receptors *in vivo* with light^{4-8,21-24}. However, neither photoswitches nor caged ligands have been shown to trigger a rapid behavioral change such as that observed here. Behavior and physiology measurements typically require a several-minute delay for drugs to diffuse and equilibrate after local administration through cannulas. The ability to present a ligand to endogenous receptors with temporal precision on the timescale of seconds is a key advantage of using photopharmacological tools *in vivo*, in addition to the spatial targeting afforded by light. Photoactivation can be paired with actions and events during behavioral experiments to study how receptor signaling in specific brain regions influences animal behavior and learning. Asking how this stimulus-response relationship is shaped by perturbing circuits and synapses (*e.g.* using chemogenetics) can then be used to study the neural circuit mechanisms of drug action. In these ways, *in vivo* photopharmacology has the potential to revolutionize behavioral pharmacology research. Although the validation of CNV-Y-DAMGO for *in vivo* studies into opioidergic neuromodulation is an important step forward, this impending paradigm shift will require the development of an extensive, pharmacologically and optically diverse toolkit of *in vivo*-compatible photopharmacological probes, as well as specialized hardware optimized for delivery of both drug and light^{25,26}.

Methods

Animal experimentation

All procedures were performed in accordance with protocols approved by the University of California San Diego Institutional Animal Care and Use Committee (IACUC) following guidelines described in the the US National Institutes of Health Guide for Care and Use of Laboratory Animals (UCSD IACUC protocol S16171). All surgery was performed under isoflurane anesthesia.

Chemical Synthesis and Characterization

DAMGO was obtained from HelloBio (HB2409) and TMSE-CNV-bromide (**6**) was synthesized according to a published procedure²⁷. All solvents were purchased as septum-sealed bottles stored under an inert atmosphere. All reactions were sealed with septa through which a nitrogen atmosphere was introduced unless otherwise noted. Reactions were conducted in round-bottomed flasks or septum-capped amber screw-cap vials containing Teflon-coated magnetic stir bars. Reactions were monitored by liquid chromatography-mass spectrometry (LC-MS) using C-18 column (4.6 × 50 mm, 1.8 μm, Agilent) with a linear gradient (water/MeCN 5%/95% → MeCN 100%, 0–8 min with 0.1% formic acid, 1 ml/min flow, electrospray ionization, positive ion mode, UV detection at 210 nm, 254 nm, and 350 nm). High-resolution mass spectrometry data were obtained at the UCSD Chemistry and Biochemistry Mass Spectrometry Facility on an Agilent 6230 time-of flight mass

spectrometer (TOFMS). Proton (^1H) and carbon (^{13}C) NMR spectra were recorded at room temperature in base-filtered CDCl_3 on a Bruker AVA-300 spectrometer operating at 300 MHz for proton and 75 MHz for carbon nuclei. For ^1H NMR spectra, signals arising from the residual protioforms of the solvent were used as the internal standards. ^1H NMR data are reported as follows: chemical shift (δ) [multiplicity, coupling constant(s) J (Hz), relative integral] where multiplicity is defined as: s = singlet; d = doublet; t = triplet; q = quartet; m = multiplet or combinations of the above. All NMR spectra were processed using MestReNova 14.2.1. UV-visible spectra were recorded on a NanoDrop 2000 UV-VIS spectrophotometer (Thermo-Fisher). Room lights were covered with Roscolux Canary Yellow #312 film (Rosco Laboratories, Stamford, CT) to filter out wavelengths of light that could lead to unintentional photolysis during purification and handling.

N-Boc-DAMGO (**5**): To a stirred solution of DAMGO (**3**) (50 mg, 97 μmol) in 1,4-dioxane/water (3/1, 300 μL) in an amber glass vial at 22 $^\circ\text{C}$, 1 M NaOH in water (97 μL , 97 μmol) was added followed by $(\text{Boc})_2\text{O}$ (21 mg, 96 μmol) in 1,4-dioxane (50 μL). The reaction was monitored by LC-MS. After 16 h, the reaction mixture was concentrated under vacuum and the residual was purified by C18 column chromatography (water/ CH_3CN , 95%/5% \rightarrow 100%). Relevant fractions were combined and concentrated under vacuum to give *N*-Boc-DAMGO as a white solid (54 mg, 90%). LR-MS (ESI) m/z 636 [(M+Na) $^+$, 100%]. HR-MS m/z 636.3005 [(M+Na) $^+$] (calcd for $\text{C}_{31}\text{H}_{43}\text{N}_5\text{O}_8\text{Na}$, 636.3004).

N-Boc-TMSE-CNV-Y-DAMGO: To an amber glass vial containing a stirred solution of *N*-Boc-DAMGO (**5**) (50 mg, 81 μmol) in anhydrous DMF (500 μL), NaH (60% in mineral oil, 3.3 mg, 82 μmol) was added slowly. The mixture was stirred at 0 $^\circ\text{C}$ for 0.5 h followed by the addition of TMSE-CNV-bromide (**6**, 34 mg, 81 μmol) in anhydrous DMF (100 μL) dropwise. The mixture was stirred under nitrogen and warmed up to 22 $^\circ\text{C}$. The reaction was monitored by LC-MS. After 3 h, a drop of MeOH was added to quench the reaction. The reaction mixture was concentrated under vacuum and the residual was purified by C18 column chromatography (water/ CH_3CN , 95%/5% \rightarrow 100%). Relevant fractions were combined and concentrated under vacuum to give *N*-Boc-TMSE-CNV-DAMGO as a white solid (67 mg, 87%). LR-MS (ESI) m/z 975 [(M+Na) $^+$, 100%]. HR-MS m/z 975.4145 [(M+Na) $^+$] (calcd for $\text{C}_{46}\text{H}_{64}\text{N}_6\text{O}_{14}\text{SiNa}$, 975.4142).

CNV-Y-DAMGO (**4**): To an amber glass vial containing a stirred solution of *N*-Boc-TMSE-CNV-DAMGO (60 mg, 63 μmol) in DCM (200 μL), TFA (400 μL) was added. The reaction was monitored by LC-MS. After 8 h, the reaction mixture was concentrated under vacuum and the residual was purified by C18 column chromatography (water/ CH_3CN , 95%/5% \rightarrow 100%) to >99.9% purity, as determined by LC-MS, and subsequently used as a mixture of diastereomers. Relevant fractions were combined and concentrated under vacuum to give CNV-Y-DAMGO as a white solid (27 mg, 58%). LR-MS (ESI) m/z 753 [(M+H) $^+$, 60%], 775 [(M+Na) $^+$, 100%]. HR-MS m/z 753.3086 [(M+H) $^+$] (calcd for $\text{C}_{36}\text{H}_{45}\text{N}_6\text{O}_{12}$, 753.3090).

***In vitro* uncaging and dark stability**

To determine dark stability, CNV-Y-DAMGO (**4**) (1 mM) was dissolved phosphate-buffered saline (PBS, pH 7.2) and left in the dark for 24 h. Comparison of samples taken at 0 and 24

h by HPLC-MS (1260 Affinity II, Agilent Technologies, Santa Clara, CA, USA) revealed no obvious decomposition or conversion to DAMGO. In addition to determining the chemical composition of the uncaging product by HPLC-MS, the initial photolysis rate of CNV-Y-DAMGO was compared to MNI-Glutamate using HPLC in response to illumination with a 375 nm laser. The concentrations of CNV-Y-DAMGO and MNI-glutamate were adjusted to match their optical densities at the photolysis wavelength of 375 nm. Solutions of CNV-Y-DAMGO (0.4 mM) and MNI-glutamate (0.5 mM) dissolved in PBS buffer (pH 7.2) were placed in 1 mL glass vials with stir bars and illuminated at a light intensity of 10 mW from a 375 nm laser (LBX-375-400-HPE-PPA, Oxixus, France) via an optical fiber (FT200UMT, 200 μ m, 0.39 NA). The solutions were illuminated in 15 sec periods, after which samples were removed and analyzed by LC-MS using a linear gradient (water/MeCN 5%/95% \rightarrow MeCN 100%, 0–8 min with 0.1% formic acid) and a (C-18 column (4.6 \times 50 mm, 1.8 μ m) (Agilent). Each compound was assessed in triplicate. The integrals of the remaining caged molecule from each sample were normalized to the integral of the un-illuminated sample, averaged and plotted against time for the first two minutes of illumination. Linear regression provided a measurement of slope, and the ratio of the two slopes was used to determine the relative photolysis efficiency of CNV-Y-DAMGO in comparison to MNI-glutamate. UV/VIS spectra were acquired on a Nanodrop One spectrophotometer (ThermoFisher)

cAMP Assay

Human embryonic kidney 293T (HEK293T) cells were grown in complete DMEM (Dulbecco's Modified Eagle's Medium (DMEM, Invitrogen, Carlsbad, CA) containing 5% fetal bovine serum (Corning), 50 U/mL Penicillin-Streptomycin (Invitrogen), and 1 mM sodium pyruvate (Corning), and maintained at 37 °C in an atmosphere of 5% CO₂ in 10 cm tissue culture (TC) dishes. When cell density reached ~70% confluence, growth medium was replaced with Opti-MEM (Invitrogen), followed by the addition of a mixture of the SSF-MOR plasmid²⁸, cAMP-dependent GloSensor reporter plasmid (–22F cAMP plasmid, Promega, E2301), and Lipofectamine 2000 (Invitrogen) in Opti-MEM. The dishes with transfection media were incubated at 37 °C in an atmosphere of 5% CO₂ for 6 h before replacing the transfection medium with complete DMEM. After incubating at 37 °C in an atmosphere of 5% CO₂ for 16 h, transfected cells were plated in poly-*D*-lysine coated 96-well plates at ~40,000 cells/well and incubated at 37 °C in an atmosphere of 5% CO₂ for 16 h. On the day of assay, the medium in each well was replaced with 50 μ L of assay buffer (20 mM HEPES, 1x HBSS, pH 7.2, 2 g/L *D*-glucose), followed by addition of 25 μ L of 4x drug (DAMGO or CNV-Y-DAMGO) solutions for 15 min at 37 °C. Finally, 25 μ L of 4 mM luciferin (Assay Reagent, Promega, E1291) supplemented with isoproterenol at a final concentration of 200 nM was added, and luminescence counting was performed after 25 min using a SpectraMax ID5 plate reader running SoftMax Pro GxP (Molecular Devices). The isoproterenol is used to increase cAMP signaling by activating endogenous Gs-coupled beta-adrenergic receptors. Pre-activation of ectopically expressed opioid receptors attenuates this cAMP signal. As such, activation of opioid receptors corresponds to low levels of isoproterenol-evoked cAMP measured in this assay. “% Activation” refers to % cAMP attenuation compared to the maximal effect of DAMGO (1 μ M).

β -arrestin recruitment assay.

HEK-293T cells were seeded on 6-well culture plates at 3×10^6 cells/well and grown in Dulbecco modified Eagle medium (DMEM; Thermo Fisher Scientific, Pittsburgh, PA, United States) supplemented with L-Glutamine 200 mM, Sodium Pyruvate 100 mM and MEM non Essential Amino Acids 100X (Biowest). 10% fetal bovine serum (FBS; Merck KGaA, Darmstadt, Germany), streptomycin (100 μ g/mL), and penicillin (100 μ g/mL) in a controlled environment (37°C, 98% humidity, and 5% CO₂). 24 h hours after seeding, cells were transfected the split NanoBit[®] vectors NB MCS1 (Promega, Madison, WI, United States) fused to human β -arrestin2 fused to the NanoBit[®]'s Lg-Bit portion at the N-terminal end of the arrestin protein or the human MOR with the Nanobit[®]'s SmBit component fused at the C-terminal end of the receptor (cytosolic side) (0.1 μ g β -arrestin2-LgBIT cDNA, 2 μ g of the hMOR-SmBIT cDNA) using polyethylenimine (PEI; Polysciences EuropeGmbH, Hirschberg an der Bergstrasse, Germany) in a 1:3 DNA:PEI ratio. 48 h after transfection, cells were rinsed, harvested, and resuspended in 4 ml/well of Hanks' Balanced Salt solution (HBSS, Sigma Aldrich, Switzerland). Cells (80 μ l/well) were then plated in 96-well white plates (PO-204003, BIOGEN) and immediately treated with increasing concentrations of DAMGO or CNV-Y-DAMGO (0.1 nM to 10 μ M), 5 min later 2 μ M coelenterazine (Prolume Ltd) was added and luminescence (490 to 410 nm) was measured during 6 min using a CLARIOstar (BMG Labtech) plate reader. β -arrestin recruitment was expressed as % of DAMGO maximum effect and concentration-response curves were fitted using Prism 9 (Graphpad Software, La Jolla, CA, USA).

Brain Slice Preparation

Animal handling protocols were approved by the UC San Diego Institutional Animal Care and Use Committee. Male and female postnatal day 15–35 mice on a C57Bl/6J background were anesthetized with isoflurane and decapitated. The brains were removed, blocked, and mounted in a VT1000S vibratome (Leica Instruments). Horizontal slices (300 μ m) were prepared in ice-cold choline-ACSF containing (in mM) 25 NaHCO₃, 1.25 NaH₂PO₄, 2.5 KCl, 7 MgCl₂, 25 glucose, 0.5 CaCl₂, 110 choline chloride, 11.6 ascorbic acid, and 3.1 pyruvic acid, equilibrated with 95% O₂/5% CO₂. Slices were transferred to a holding chamber containing oxygenated artificial cerebrospinal fluid (ACSF) containing (in mM) 127 NaCl, 2.5 KCl, 25 NaHCO₃, 1.25 NaH₂PO₄, 2 CaCl₂, 1 MgCl₂, and 10 glucose, osmolarity 290. Slices were incubated at 32 °C for 30 min and then left at room temperature until recordings were performed.

Electrophysiology

All recordings were performed within 5 h of slice cutting in a submerged slice chamber perfused with ACSF warmed to 32 °C and equilibrated with 95% O₂/5% CO₂. Whole-cell voltage clamp recordings were made with an Axopatch 700B amplifier (Axon Instruments). Data were sampled at 10 kHz, filtered at 3 kHz, and acquired using National Instruments acquisition boards and a custom version of ScanImage written in MATLAB (Mathworks)²⁹. Cells were rejected if holding currents were more negative than –200 pA or if the series resistance (<20 M Ω) changed during the experiment by more than 20%. Patch

pipettes (2.5–3.5 M Ω) were filled with an internal solution containing (in mM) 135 CsMeSO₃, 10 HEPES, 1 EGTA, 3.3 QX-314 (Cl⁻ salt), 4 Mg-ATP, 0.3 Na-GTP, and 8 Na₂ phosphocreatine (pH 7.3, 295 mOsm/kg). Cells were held at 0 mV to produce outward inhibitory currents. Excitatory transmission was blocked by the addition to the ACSF of NBQX (10 μ M) and CPP (10 μ M). To electrically evoke IPSCs, stimulating electrodes pulled from theta glass with ~5 μ m tip diameters were placed at the border between stratum pyramidale and stratum oriens nearby the recorded cell (~50–150 μ m) and two brief pulses (0.5 ms, 50–300 μ A, 50 ms interval) were delivered every 20 s.

Ex vivo UV Photolysis

Uncaging was carried out during brain slice electrophysiology recordings using 5 ms flashes of collimated full-field illumination with a 355 nm laser using a custom light path, as previously described¹⁰. Light power in the text (84 mW) correspond to measurements of a 10 mm diameter collimated beam at the back aperture of the objective. Beam size exiting the objective onto the sample through a 60x objective was 3900 μ m². Caged peptide was circulated in ACSF at the indicated concentrations at a flow rate of 4 ml/min using a peristaltic pump.

In vivo UV Photolysis

Formalin assay of inflammatory pain.

Male postnatal day 40 mice on a C57Bl/6J background were implanted unilaterally with an Optical Fiber Multiple Fluid Injection Cannula (OmFC, Doric Lenses) just above the left nucleus accumbens medial shell at the following coordinates (in mm, from bregma): AP 1.54, ML -0.5, DV -4.3. Only male mice were used, as preliminary experiments suggested that female mice may be less responsive to NAc-mSh opioids in this assay. The fluid guide cannula (485 μ m OD) length was 4.5 mm, the flat tip (FLT) optical fiber (200 μ m, 0.22 NA) length was 4.8 mm, the optical fiber receptacle was a 1.25 mm zirconia ferrule (ZF1.25), and the fluid injector (170 μ m OD, 100 μ m ID) length was 5.0 mm. Mice were allowed to recover for at least 5 days post-surgery and acclimated to the room and experimenter for several days prior to experimentation. Mice were brought to the room ~30 min prior to the start of each experiment. The optical fiber was coupled to a fiber optic cable (200 μ m, 0.22 NA) connected to a 375 nm laser (Vortran Stradus), which was controlled by an Arduino Uno using a custom code to control pulse duration and frequency. A syringe pump (WPI) was connected via flexible silicon tubing to a fluid injector loaded with CNV-Y-DAMGO (200 μ M) and the fluid injector was connected to the optofluidic cannula. Mice were injected in their right hindpaw with formalin (2.5 %, 20 μ L) and placed into a clear round cylinder. Nocifensive responses were video recorded with side-view cameras placed on opposite sides of the cylinder. 10 min after formalin injection, CNV-Y-DAMGO was infused for 5 min at a flow rate of 0.1 μ L/min. The tubing was not disconnected when the infusion ceased. 15 min later, light flashes (10 \times 200 ms, 1 Hz, 70 mW) were applied, after which mice were observed for an additional 30 min. Reported light power refers to measurements from the ferrule tip of the laser-coupled optical fiber (200 μ m, 0.22 NA) that connects to the implanted fiber. Tethered control mice containing implants in the prefrontal cortex were

connected to the same fiber optic cable. They were not connected to a syringe pump and no light was applied.

Locomotion.

Male and female postnatal day 40 mice on a C57Bl/6J background were implanted unilaterally with an Optical Fiber Multiple Fluid Injection Cannula (same dimensions as used for the NAc-mSh) just above the left ventral tegmental area at the following coordinates (in mm, from bregma): AP -3.33, ML -0.5, DV -4.15 at a 10° M/L angle. Mice were allowed to recover for at least 5 days post-surgery and acclimated to the room and experimenter for several days prior to experimentation. Mice were brought to the room ~30 min prior to the start of each experiment. Using a syringe pump connected to the fluid injector, CNV-Y-DAMGO (200 µM) was infused for 5 min at a flow rate of 0.1 µL/min. Mice were allowed to move freely for the duration of drug delivery. The fluid injector was allowed to remain in place for 1 min following infusion, after which the dummy fluid injector was reinserted. The optical fiber was coupled to a fiber optic cable (200 µm, 0.22 NA) connected to an Arduino-controlled 375 nm laser. Mice were placed in a square enclosure (18 × 18 cm) where their position was video recorded at a 30 fps using a webcam (Logitech) fed into Smart 3.0 video tracking software (Panlab). Following a 15 min baseline period, the indicated number of light flashes (200 ms, 1 Hz) were applied at the indicated powers, after which mice were tracked for an additional 25 min. In some experiments CNV-Y-DAMGO was replaced with saline only, the light flashes were omitted, or naloxone (3 mg/kg, intraperitoneal) was administered immediately before beginning the infusion.

Histology

Mice were anesthetized with isoflurane via the open drop method and perfused with 20 mL of PBS, followed by 20 ml of chilled 4% PFA in 1x PBS. The brains were collected, placed in 4% PFA overnight at 4°C, and transferred to a 30% sucrose solution for at least 18 h prior to sectioning. Brains were sliced into 40 µm sections using a sliding microtome (Thermo Scientific Microm HM 450) and collected in PBS in 24-well plates. Sections selected for immunohistochemistry were blocked in PBS-Triton (0.3% TritonX-100 in 1x PBS) + 5% donkey serum for 2 h at room temperature. The sections were then incubated with rabbit anti-tyrosine hydroxylase (Millipore, AB152; 1:1000) in PBS-Triton + 1% donkey serum at 4°C overnight while shaking. Following primary incubation, sections were washed 5x at 10 min per wash in PBS, then incubated with Alexa Fluor 647 donkey anti-rabbit IgG (Invitrogen; 1:1000) in PBS-Triton + 1% donkey serum for 2 h at room temperature for secondary staining. Following secondary incubation, sections were washed 5x at 10 min each in PBS, then mounted on glass slides using Vectashield Antifade Mounting Medium with DAPI (H-1200). Images of the slices were acquired on a Keyence (BZ-X710 series) at 10x magnification.

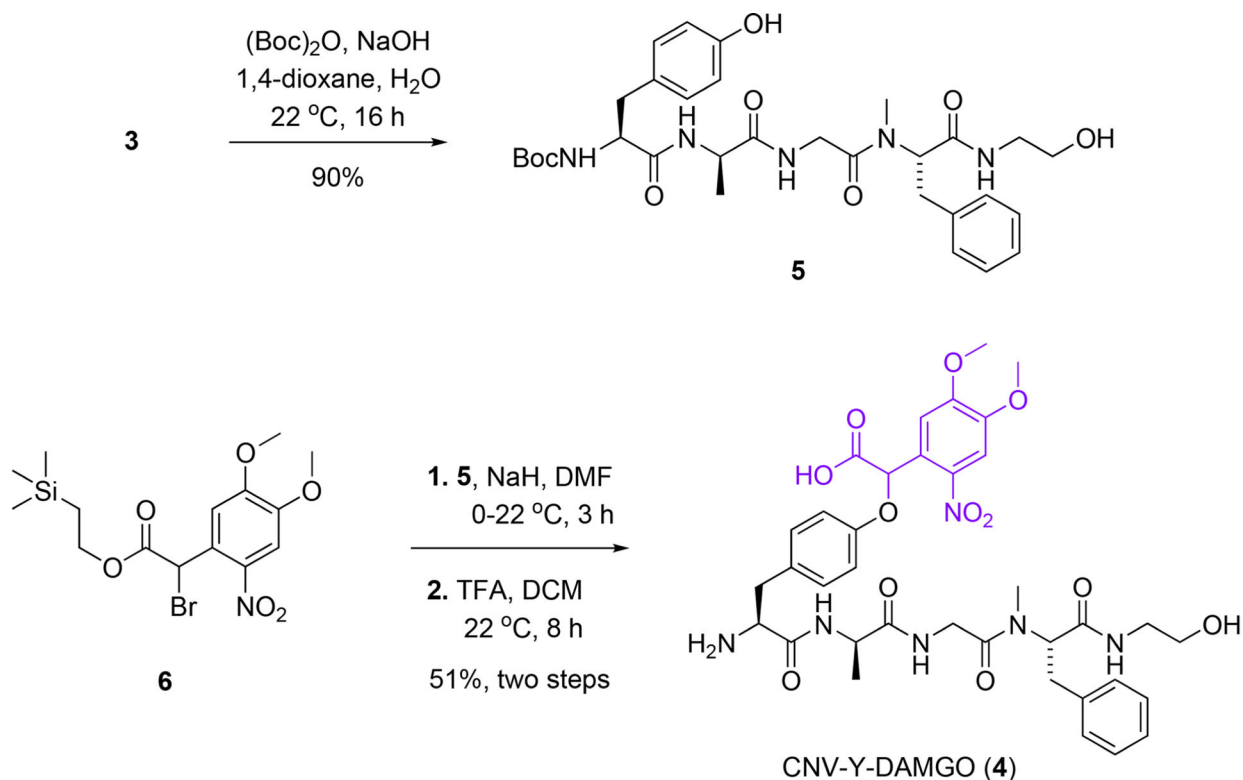
Data Analysis

Electrophysiology data were processed using Igor Pro (Wavemetrics). Peak current amplitudes were calculated by averaging over a 2 ms window around the peak of the average IPSC recorded from each cell. To determine the magnitude of modulation by DAMGO

uncaging (%IPSC suppression), the IPSC peak amplitude immediately after a flash was divided by the average peak amplitude of the three IPSCs preceding the light flash. The effects of drugs on IPSC suppression were calculated as the average % IPSC suppression 2–3 min after drug addition. For *in vivo* uncaging experiments involving the formalin assay, nocifensive responses including licking, shaking, and guarding the right hindpaw contralateral to the photostimulation site were manually quantified post-hoc.

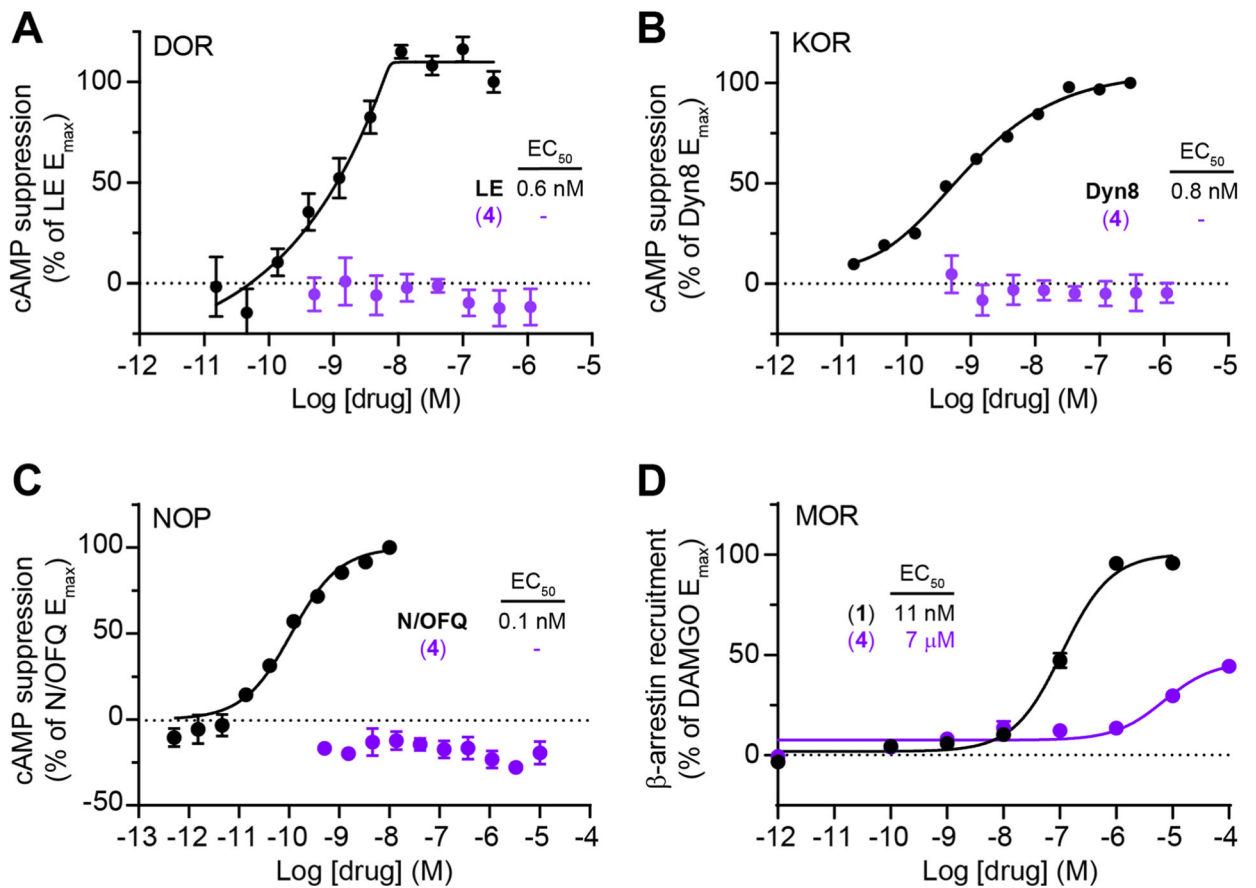
For locomotor analysis, video measurements of mouse position over time were analyzed in either 5 or 1 s bins for instantaneous velocity determination, and in 15 min bins before and after uncaging for calculating total distance traveled (Smart 3.0 video tracking software, Panlab). All processed data were subsequently analyzed and plotted using GraphPad Prism v9.3.1. The Shapiro-Wilk test was used to determine that datasets to be analyzed follow a normal distribution. Either a two-tailed t-test (unpaired or paired), or a two-tailed Mann Whitney test was used to determine p values, as described in the figures and corresponding legends.

Extended Data



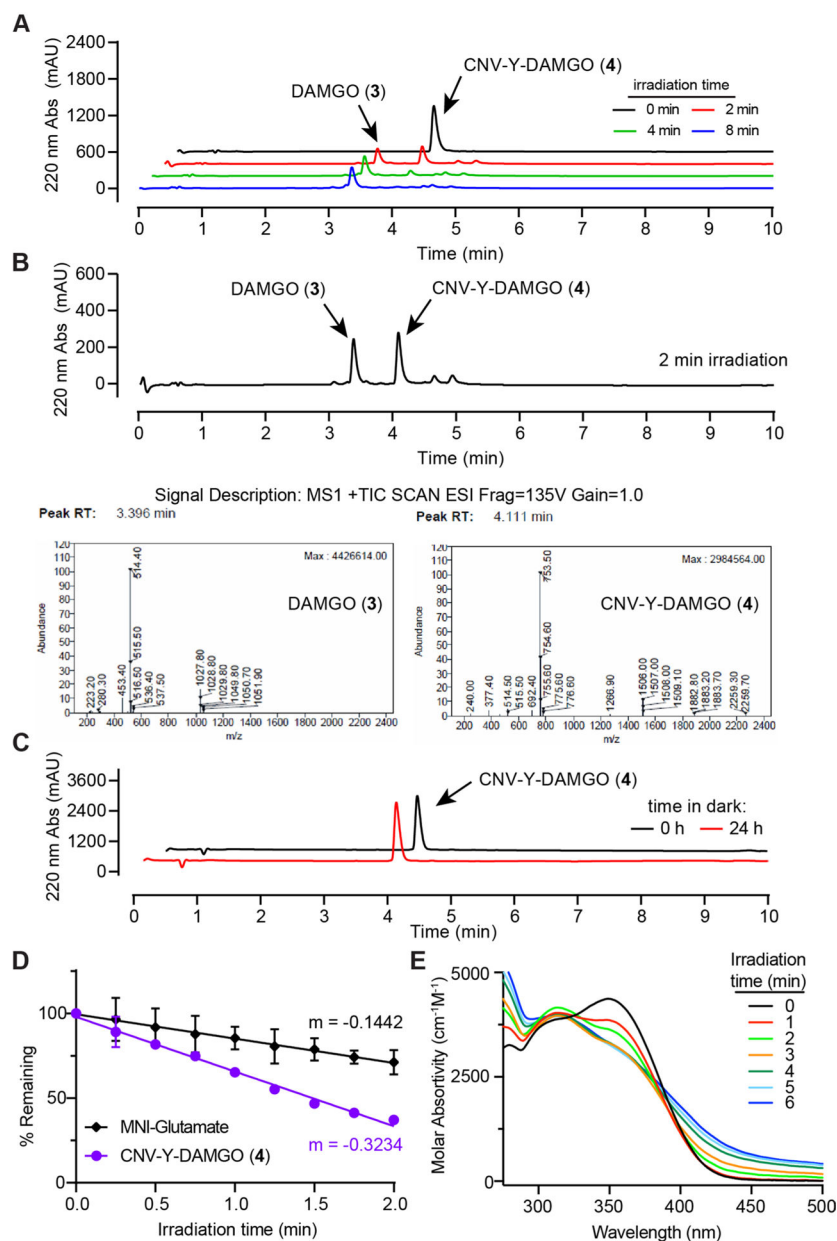
Extended Data Fig. 1 |. Synthesis of CNV-Y-DAMGO (4).

The N-terminal amine in DAMGO (**3**) was Boc-protected prior to phenol alkylation with **6**. Global deprotection with TFA produced CNV-Y-DAMGO (**4**) in good overall yield



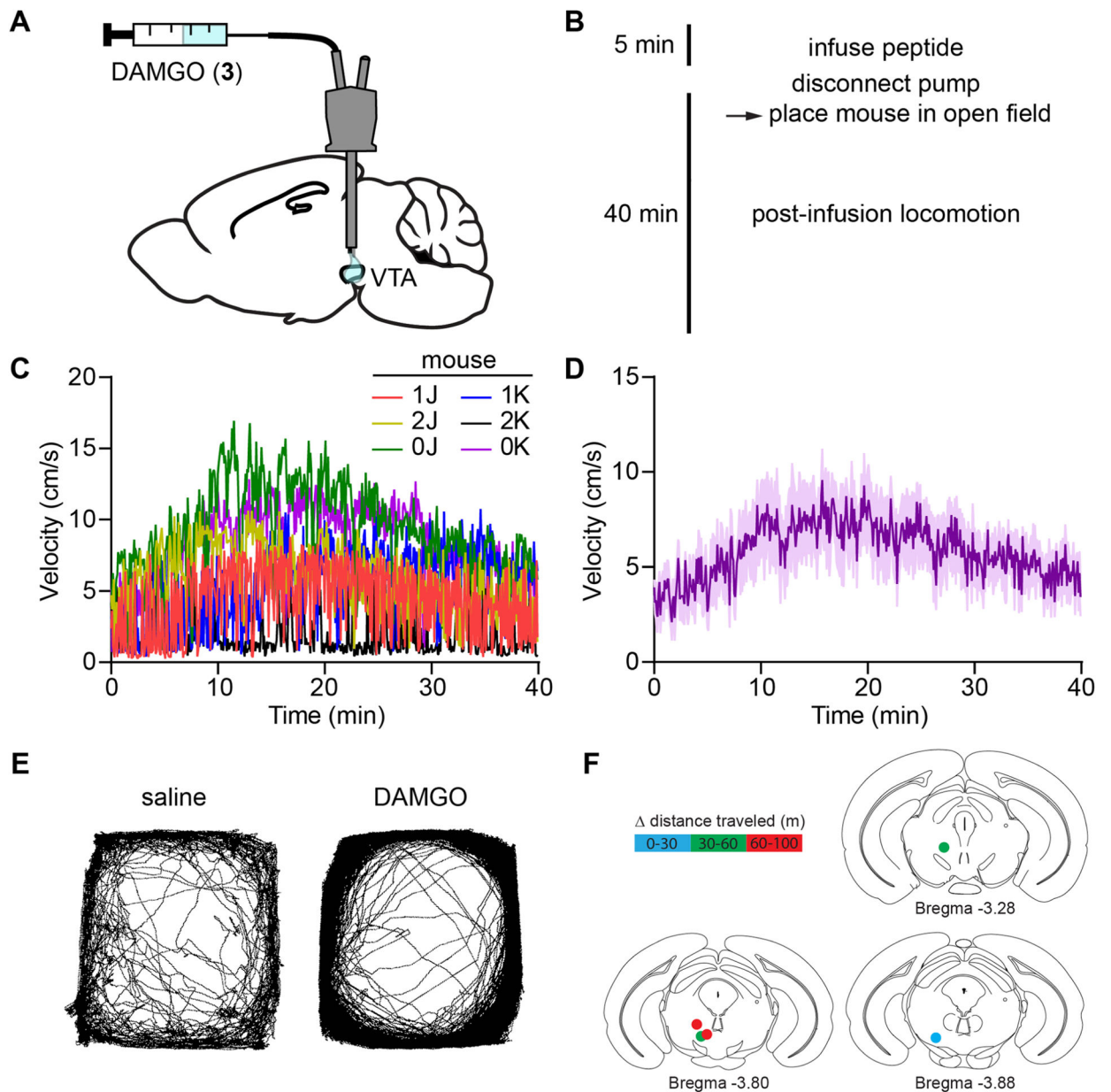
Extended Data Fig. 2 | In vitro characterization of CNV-Y-DAMGO activity at opioid receptors.

(A) Dose-response curves at the delta opioid receptor (DOR) using a GloSensor assay of cAMP signaling in HEK293T cells ($n = 5$ wells per data point, 1 representative independent experiment shown). Data were normalized to the maximal response to leucine-enkephalin (LE, 1 μ M) and are expressed as the mean \pm SEM. (B) Same as A, but using the kappa opioid receptor (KOR) and dynorphin A(1–8) (Dyn8, 1 μ M) for normalization. (C) Same as A, but using the nociceptin/orphanin FQ receptor (NOP) and nociception/orphanin FQ (N/OFQ, 1 μ M) for normalization. (D) Dose-response curves at the mu opioid receptor (MOR) using a NanoBiT-based luminescence complementation assay of β -arrestin signaling in HEK293T cells ($n = 4$ wells per data point, 3 independent experiments averaged). Data were normalized to the maximal response to DAMGO (10 μ M) and are expressed as the mean \pm SEM.



Extended Data Fig. 3 | In vitro characterization of CNV-Y-DAMGO (4) photolysis and dark stability.

(A) Waterfall plot of HPLC chromatograms of CNV-Y-DAMGO (0.4 mM) during illumination with 375 nm light (10 mW) in PBS, pH 7.2. (B) Enlarged HPLC chromatogram after 2 min of illumination (top) and mass spectrograms corresponding to the indicated peaks (bottom). (C) HPLC chromatograms of a sample of CNV-Y-DAMGO (1 mM) in PBS left for 24 hours in the dark. (D) Summary of MNI-Glutamate and CNV-Y-DAMGO photouncaging reactions over time, as measured by HPLC ($n = 3$ samples per condition). Samples were optical density-matched at 375 nm in PBS and illuminated with 375 nm laser irradiation. Data are expressed as the mean \pm SEM. (E) UV-VIS spectrum of samples of CNV-Y-DAMGO (0.4 mM) in PBS before and after irradiation with 375 nm light (10 mW) for the indicated time periods.



Extended Data Fig. 4 | DAMGO infusion into the VTA and location of optofluidic cannula placements.

(A) Schematic of the experimental configuration for DAMGO infusion through an optofluidic cannula. (B) Experimental timeline. (C) Movement velocity vs. time in the open field for a cohort of mice after DAMGO (200 μ M, 0.5 μ L) infusion. (D) Average data from C (n = 6 mice). Data are expressed as the mean \pm SEM. (E) Example maps of open field locomotor activity from a single mouse after infusion of either saline or DAMGO. (F) Change in distance traveled (after-before uncaging) mapped to the implant location for the mice shown in Fig. 2g,h.

Supplementary Material

Refer to Web version on PubMed Central for supplementary material.

Acknowledgements

We thank Eric Berg for technical support, Jeffrey Isaacson for helpful discussions, and Janie Chang-Weinberg for manuscript editing. This work was supported by the National Institute of Neurological Disorders and Stroke and the National Institute of Mental Health (U01NS113295 to M.R.B.), the National Institute of General Medical Sciences (R35GM133802 to M.R.B., T32GM007240 to X.J.H.), the Brain & Behavior Research Foundation (M.R.B.), the Esther A. & Joseph Klingenstein Fund & Simons Foundation (M.R.B.), the Rita Allen Foundation (M.R.B.), and by Plan Nacional Sobre Drogas (Spanish Ministerio de Sanidad, 20211070 to J.B.).

Data Availability

The data supporting the findings of this study are available within the paper and its Extended Data files. Source data are provided with this paper.

References

1. Ellis-Davies GCR Caged compounds: photorelease technology for control of cellular chemistry and physiology. *Nat. Methods* 4, 619–628 (2007). [PubMed: 17664946]
2. Paoletti P, Ellis-Davies GCR & Mouroto A Optical control of neuronal ion channels and receptors. *Nat. Rev. Neurosci* 20, 514–532 (2019). [PubMed: 31289380]
3. Ankenbruck N, Courtney T, Naro Y & Deiters A Optochemical Control of Biological Processes in Cells and Animals. *Angewandte Chemie - International Edition* 57, 2768–2798 (2018). [PubMed: 28521066]
4. Font J et al. Optical control of pain in vivo with a photoactive mGlu5 receptor negative allosteric modulator. *Elife* 6, (2017).
5. López-Cano M et al. Remote local photoactivation of morphine produces analgesia without opioid-related adverse effects. *Br. J. Pharmacol* (2021). doi:10.1111/bph.15645
6. Cuttoli R. D. De et al. Optofluidic control of rodent learning using cloaked caged glutamate. *Proc. Natl. Acad. Sci. U. S. A* 117, 6831–6835 (2020). [PubMed: 32152102]
7. Taura J et al. Remote control of movement disorders using a photoactive adenosine A 2A receptor antagonist. *J. Control. Release* 283, 135–142 (2018). [PubMed: 29859955]
8. Noguchi J et al. In vivo two-photon uncaging of glutamate revealing the structure-function relationships of dendritic spines in the neocortex of adult mice. *J. Physiol* 589, 2447–2457 (2011). [PubMed: 21486811]
9. Gomes I et al. Biased signaling by endogenous opioid peptides. *Proc. Natl. Acad. Sci. U. S. A* 117, (2020).
10. Banghart MR & Sabatini BL Photoactivatable neuropeptides for spatiotemporally precise delivery of opioids in neural tissue. *Neuron* 73, 249–59 (2012). [PubMed: 22284180]
11. Banghart MR, He XJ & Sabatini BL A Caged Enkephalin Optimized for Simultaneously Probing Mu and Delta Opioid Receptors. *ACS Chem. Neurosci* 9, 684–690 (2018). [PubMed: 29266926]
12. Craves FB, Law PY, Hunt CA & Loh HH The metabolic disposition of radiolabeled enkephalins in vitro and in situ. *J. Pharmacol. Exp. Ther* 206, 492–506 (1978). [PubMed: 682128]
13. Handa BK et al. Analogues of β -LPH61–64 possessing selective agonist activity at μ -opioid receptors. *Eur. J. Pharmacol* 70, 531–540 (1981). [PubMed: 6263640]
14. He XJ et al. Convergent, functionally independent signaling by mu and delta opioid receptors in hippocampal parvalbumin interneurons. *Elife* 10, (2021).
15. Castro DC et al. An endogenous opioid circuit determines state-dependent reward consumption. *Nature* 598, 646–651 (2021). [PubMed: 34646022]

16. Manning BH, Morgan MJ & Franklin KBJ Morphine analgesia in the formalin test: Evidence for forebrain and midbrain sites of action. *Neuroscience* 63, 289–294 (1994). [PubMed: 7898653]
17. Johnson SW & North RA Opioids excite dopamine neurons by hyperpolarization of local interneurons. *J. Neurosci* 12, 483–488 (1992). [PubMed: 1346804]
18. Joyce EM & Iversen SD The effect of morphine applied locally to mesencephalic dopamine cell bodies on spontaneous motor activity in the rat. *Neurosci. Lett* 14, 207–212 (1979). [PubMed: 530497]
19. Hüll K, Morstein J & Trauner D In Vivo Photopharmacology. *Chemical Reviews* 118, 10710–10747 (2018). [PubMed: 29985590]
20. Tochitsky I, Kienzler MA, Isacoff E & Kramer RH Restoring Vision to the Blind with Chemical Photoswitches. *Chemical Reviews* 118, 10748–10773 (2018). [PubMed: 29874052]
21. Gomila AMJ et al. Photocontrol of Endogenous Glycine Receptors In Vivo. *Cell Chem. Biol* 27, 1425–1433.e7 (2020). [PubMed: 32846115]
22. Donthamsetti P et al. Cell specific photoswitchable agonist for reversible control of endogenous dopamine receptors. *Nat. Commun* 12, (2021).
23. Acosta-Ruiz A et al. Branched Photoswitchable Tethered Ligands Enable Ultra-efficient Optical Control and Detection of G Protein-Coupled Receptors In Vivo. *Neuron* 105, 446–463.e13 (2020). [PubMed: 31784287]
24. Davenport CM et al. Relocation of an Extrasynaptic GABAA Receptor to Inhibitory Synapses Freezes Excitatory Synaptic Strength and Preserves Memory. *Neuron* 109, 123–134.e4 (2021). [PubMed: 33096025]
25. Zhang Y et al. Battery-free, lightweight, injectable microsystem for in vivo wireless pharmacology and optogenetics. *Proc. Natl. Acad. Sci. U. S. A* 116, 21427–21437 (2019). [PubMed: 31601737]
26. Frank JA et al. In Vivo Photopharmacology Enabled by Multifunctional Fibers. *ACS Chem. Neurosci* 11, 3802–3813 (2020). [PubMed: 33108719]
27. Gilbert D et al. Caged capsaicins: New tools for the examination of TRPV1 channels in somatosensory neurons. *ChemBioChem* 8, 89–97 (2007). [PubMed: 17154194]
28. Tanowitz M & Von Zastrow M A Novel Endocytic Recycling Signal That Distinguishes the Membrane Trafficking of Naturally Occurring Opioid Receptors. *J. Biol. Chem* 278, 45978–45986 (2003). [PubMed: 12939277]
29. Pologruto TA, Sabatini BL & Svoboda K ScanImage: Flexible software for operating laser scanning microscopes. *Biomed. Eng. Online* 2, (2003).

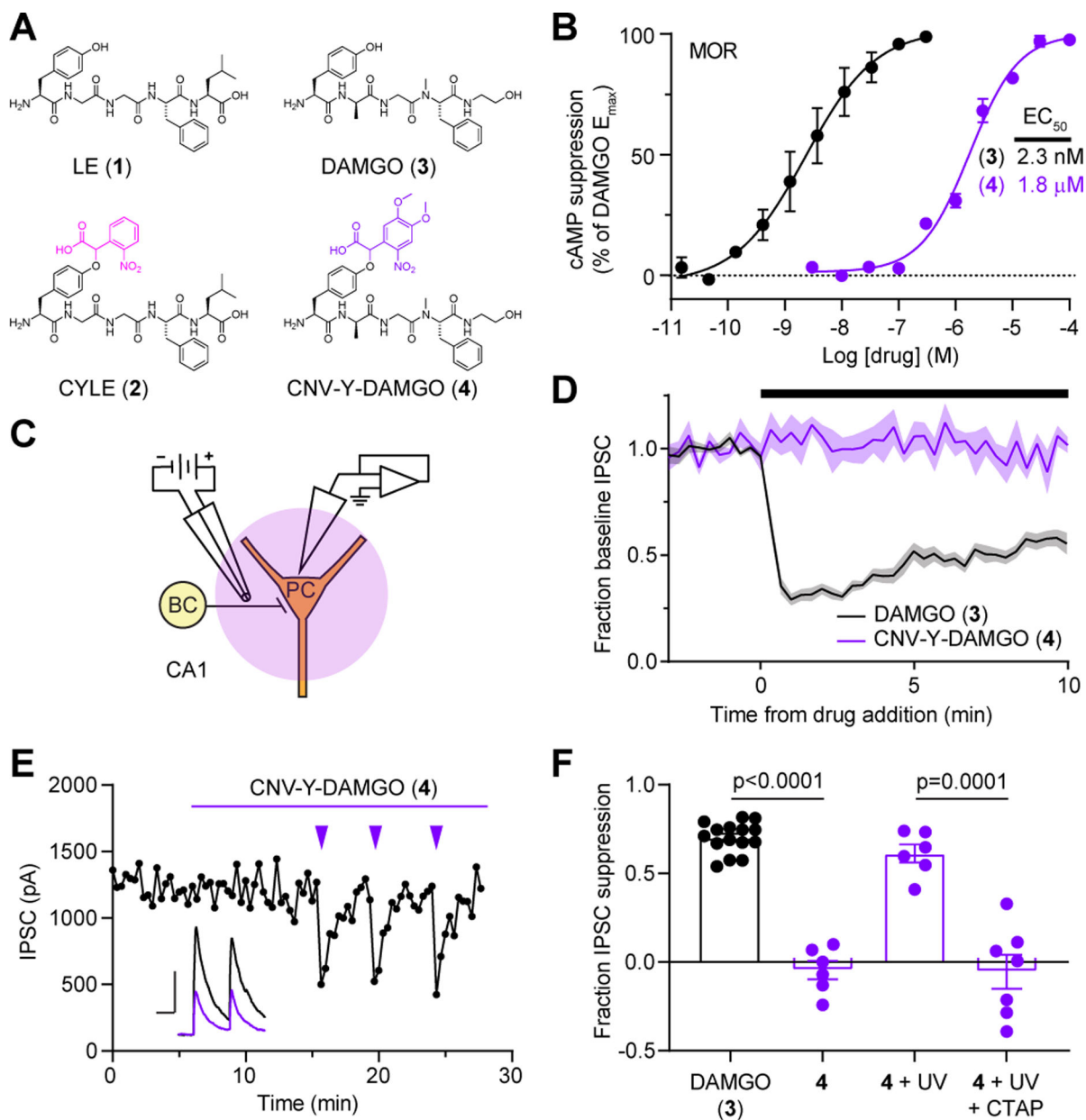


Figure 1. Design and validation of CNV-Y-DAMGO *in vitro* and *ex vivo*.

(A) Design of a caged DAMGO based on caged [Leu⁵]-enkephalin. (B) Dose-response curves were obtained using a GloSensor assay of cAMP signaling in HEK293T cells (n=3 experimental replicates, each run in quintuplicate). Data were normalized to the maximal response to DAMGO (1 μ M) and are expressed as the mean \pm SEM. (C) Schematic of the experimental configuration for photouncaging of CNV-Y-DAMGO while recording electrically-evoked inhibitory synaptic transmission from CA1 hippocampal basket cells (BC) impinging on pyramidal cells (PC). (D) Baseline-normalized, average inhibitory post-synaptic current (IPSC) amplitude over time during bath application of DAMGO (1 μ M, n = 15 cells from 14 mice) or CNV-Y-DAMGO (1 μ M, n = 6 cells from 4 mice). Data are expressed as the mean \pm SEM. (E) Representative example of IPSC amplitude over

time during bath application of CNV-Y-DAMGO (1 μ M) and repeated photolysis using 355 laser flashes (84 mW, 5 ms). **Inset:** Example IPSCs immediately before (black) and after (purple) CNV-Y-DAMGO uncaging. Scale bars: \times = 25 ms, y = 500 pA. **(F)** Summary data comparing the fraction of baseline IPSC suppression in response to either DAMGO (1 μ M) bath application, CNV-Y-DAMGO (1 μ M) bath application, CNV-Y-DAMGO uncaging, and CNV-Y-DAMGO uncaging in the presence of the mu-selective antagonist CTAP (1 μ M) (DAMGO (n = 15 cells from 14 mice), CNV-Y-DAMGO (n = 6 cells from 4 mice), CNV-Y-DAMGO + UV (n = 6 cells from 4 mice), CNV-Y-DAMGO + UV + CTAP (n = 7 cells from 2 mice)). P values were determined using a two-tailed unpaired t-test. Data are expressed as the mean \pm SEM.

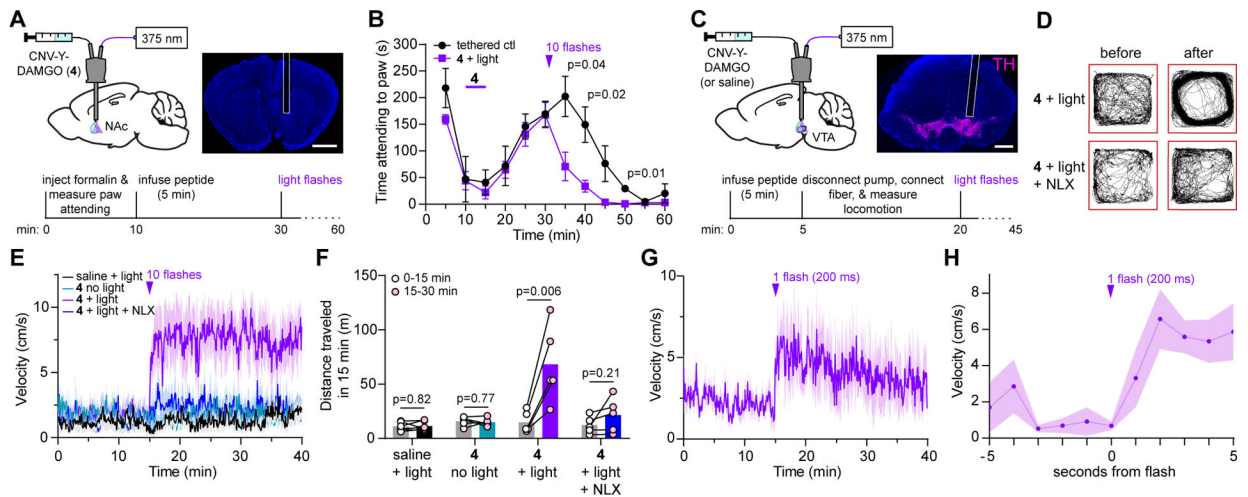


Figure 2. *In vivo* uncaging with CNV-Y-DAMGO modulates pain-related behavior and locomotion.

(A) Schematic of the experimental configuration for photo-uncaging through an optofluidic cannula in the NAc-mSh (top left), example image of cannula placement above the NAc-mSh (top right, scale bar = 1 mm), and experimental timeline for uncaging during the formalin assay (bottom). (B) Average time spent attending to the inflamed paw for a cohort of tethered control mice (n=4 mice) and mice treated with CNV-Y-DAMGO and light (n=6 mice). The time of the uncaging stimulus is indicated by the purple arrowhead. P values were determined using a two-tailed Mann Whitney test. Data are expressed as the mean \pm SEM. (C) Schematic of the experimental configuration for photo-uncaging in the VTA (top left), example image of cannula placement above the VTA, indicated by immunohistochemical labeling of tyrosine hydroxylase (TH, top right, scale bar = 1 mm), and experimental timeline for uncaging in the open field (bottom). (D) Example maps of open field locomotor activity from a single mouse before and after uncaging. (E) Average movement velocity vs. time for a cohort of mice treated with either saline and light (10 flashes, n=6 mice), CNV-Y-DAMGO without light (n = 5 mice), CNV-Y-DAMGO with light (n = 5 mice), and CNV-Y-DAMGO with light in the presence of the opioid antagonist naloxone (NLX) (n = 5 mice). Data are expressed as the mean \pm SEM. (F) Summary data of distance traveled in the 15 minutes before and after application of the 10-flash uncaging stimulus (from the data shown in E). P values were determined using a two-tailed paired t-test. (G) Average movement velocity vs. time upon exposure to a single light flash (n = 5 mice). Data are expressed as the mean \pm SEM. (H) Same data as in G, but sampled at 1 Hz and zoomed in around the uncaging stimulus. Data are expressed as the mean \pm SEM.